

Computation of the expected value of a function of a chi-distributed random variable

Paul Kabaila and Nishika Ranathunga

Department of Mathematics and Statistics, La Trobe University,
Victoria 3086, Australia

Abstract

We consider the problem of numerically evaluating the expected value of a smooth bounded function of a chi-distributed random variable, divided by the square root of the number of degrees of freedom. This problem arises in the contexts of simultaneous inference, the selection and ranking of populations and in the evaluation of multivariate t probabilities. It also arises in the assessment of the coverage probability and expected volume properties of the non-standard confidence regions considered Kabaila and co-authors. We propose the application of the “Mixed Rule” transformation, followed by the application of the trapezoidal rule. This rule has the remarkable property that, for suitable integrands, it is exponentially convergent. We use it to create a nested sequence of quadrature rules, for the estimation of the approximation error, so that previous evaluations of the integrand are not wasted. The application of the trapezoidal rule requires the approximation of an infinite sum by a finite sum. We provide a new easily computed upper bound on the error of this approximation. Our overall conclusion is that this method is very suitable for the assessment of the coverage and expected volume properties of non-standard confidence regions.

Keywords: Confidence interval; Coverage probability; Mixed rule transformation; Numerical integration; Trapezoidal rule

1 Introduction

Consider the problem of finding an accurate and efficient method of numerically computing an integral of the form

$$\int_0^\infty a(x) f_\nu(x) dx, \quad (1)$$

where a is a smooth bounded real-valued function, ν is a positive integer and f_ν is the probability density function (pdf) of a random variable with the same distribution as $R/\nu^{1/2}$, where R has a χ_ν distribution (i.e. R^2 has a χ_ν^2 distribution). Note that (1) = $E(a(R/\nu^{1/2}))$, which is the expected value of a smooth bounded function of $R/\nu^{1/2}$. We suppose that a computer program for the accurate and efficient evaluation of $a(x)$, for any given $x > 0$, is either already available or can be easily written. In other words, our focus is solely on the numerical evaluation of the integral (1).

The evaluation of an integral of this form occurs in the context of simultaneous statistical inference and the selection and ranking of populations (Miller 1981; Hochberg and Tamhane 1987; Gupta and Panchapakesan 2002) and in the evaluation of central and non-central (Kshirsagar definition) multivariate t probabilities (Dunnett and Sobel 1955; Dunnett 1989; Genz and Bretz 2009), when the method of Miwa et al. (2003), briefly described in Mi et al. (2009), is used to compute $a(x)$.

The evaluation of an integral of the form (1) also occurs in the computation of the coverage probabilities of post-model-selection confidence intervals, frequentist model averaged confidence intervals and other non-standard confidence regions (Farchione and Kabaila 2008; Kabaila and Farchione 2012; Kabaila et al. 2016; Kabaila et al. 2017; Abeysekera and Kabaila 2017; Kabaila 2018). In all of these papers, this evaluation has previously been carried out by first truncating the integral (the truncation error is easily bounded) and then applying an adaptive numerical integration method.

Our search for a better method for the evaluation of an integral of the form (1) has led us to apply the “Mixed Rule” transformation described by Press et al. (2007, p.176), followed by application of the trapezoidal rule over the real line. This transformation belongs to a family of transformations proposed and investigated by Takahasi and Mori (1973), Mori (1985) and others. The trapezoidal rule has the remarkable property that, for suitable integrands, it is exponentially convergent (Trefethen and Weideman 2014). There are several well-known explanations for this remarkable property, including the Euler-Maclaurin summation formula and Fourier transform methods. A historical review of the these explanations is provided in Section 11 of Trefethen and Weideman (2014). The trapezoidal rule also has the great

advantage that it can be used to create a nested sequence of quadrature rules, used for the estimation of the approximation error, so that previous evaluations of the function a are not wasted.

For our purposes, the best description of the properties of the trapezoidal rule is found using the Fourier transform of the integrand and the Poisson summation formula. For the reader's convenience, this well-known description is recounted in Section 2. The application of the "Mixed Rule" transformation to the integral (1), followed by the application of the trapezoidal rule is described in Section 3. In this section, our main contribution is to describe a method of carrying out the required truncation of the infinite sum approximation to the integral that leads to an easily-computed upper bound on the resulting truncation error.

In Section 4 we use the simple test scenario that consists of evaluating a known univariate t probability (i.e the value of (1) is known). We compare the performance of the method described in Section 3 with the following two methods:

1. Generalized Gauss Laguerre quadrature

Change the variable of integration in (1) to $y = \nu x^2/2$. In effect, we express the expectation of interest, $E(a(R/\nu^{1/2}))$, as $E(a(2^{1/2} V^{1/2}/\nu^{1/2}))$, where $V = R^2/2$ has a $\text{gamma}(\nu/2, 1)$ distribution. We then apply Generalized Gauss Laguerre quadrature.

2. Inverse cdf method

Change the variable of integration in (1) to $y = F_\nu(x)$, where F_ν denotes the cumulative distribution function (cdf) that corresponds to the pdf f_ν . This transforms the integral (1) into an integral over the interval $[0, 1]$. In effect, we express the expectation of interest, $E(a(R/\nu^{1/2}))$, as $E(a(F_\nu^{-1}(U)))$, where $U = F_\nu(R/\nu^{1/2})$ is uniformly distributed on $(0, 1)$. We then apply Gauss Legendre quadrature.

The purpose of this comparison is to illustrate the factors that may lead to a relatively poor performance of these two methods. The computations for this paper were carried out using the R computer language.

Finally, in Section 5 we discuss the application of the method described in Section 3 to the computation of the coverage probability and scaled expected length of of post-model-selection and frequentist model averaged confidence intervals. We also consider the application of this method to the computation of the coverage probability and scaled expected volume of other non-standard confidence regions.

2 Properties of the trapezoidal rule found using the Fourier transform of the integrand

Suppose that we wish to evaluate

$$\int_{-\infty}^{\infty} g(y) dy, \quad (2)$$

where g is a real-valued absolutely integrable function. Let G denote that Fourier transform of g . This transform is defined by

$$G(\omega) = \int_{-\infty}^{\infty} g(y) \exp(-i\omega y) dy,$$

where $i = \sqrt{-1}$ and the angular frequency $\omega \in \mathbb{R}$. Since g is real-valued, $G(\omega)$ is an even function of ω (see e.g. p.11 of Papoulis 1962). It follows from the Poisson summation formula (see e.g. p.47 of Papoulis 1962) that

$$\left| h \sum_{j=-\infty}^{\infty} g(jh + \delta) - \int_{-\infty}^{\infty} g(y) dy \right| \leq 2 \sum_{j=1}^{\infty} \left| G\left(\frac{2\pi j}{h}\right) \right|, \quad (3)$$

for all $\delta \in [0, h)$. The left-hand side is the magnitude of the *discretization error*. This magnitude is small when $|G(\omega)|$ decays rapidly as $\omega \rightarrow \infty$ and h is sufficiently small.

We approximate the infinite sum

$$h \sum_{j=-\infty}^{\infty} g(jh + \delta) \quad (4)$$

by the finite sum

$$h \sum_{j=M}^N g(jh + \delta), \quad (5)$$

for appropriately chosen integers M and N ($M < N$). The “trapezoidal rule” approximation to (2) is (5). The difference (5) – (4) is called the *trimming error*. The difference (4) – (2) is called the *discretization error*. For (5) to be a good approximation to (2), we require that the magnitudes of both the *discretization error* and the *trimming error* are small. As noted by Press et al. (2007), “the optimal strategy is to try to arrange that the magnitudes of the discretization and trimming errors are approximately equal”.

The “uncertainty principle” for Fourier transforms, given e.g. on p.63 of Papoulis (1962), and the theorem of Hardy (1933), described on p.717

of Press et al. (2007), suggest that the trapezoidal rule can be made to be particularly efficient for g proportional to the pdf of a normally distributed random variable. This, in turn, suggests the heuristic that the trapezoidal rule can be made to be efficient when g has some resemblance to such a function.

3 The “Mixed Rule” transformation of (1), followed by the application of the trapezoidal rule

The pdf f_ν is given by

$$f_\nu(x) = \begin{cases} \frac{\nu^{\nu/2}}{\Gamma(\nu/2) 2^{(\nu/2)-1}} x^{\nu-1} \exp(-\nu x^2/2) & \text{for } x > 0 \\ 0 & \text{otherwise.} \end{cases}$$

To evaluate (1), we first apply the “Mixed Rule” transformation $x(y) = \exp(y - e^{-y})$, so that

$$\frac{dx(y)}{dy} = \exp(y - e^{-y}) (1 + e^{-y})$$

and

$$\int_0^\infty a(x) f_\nu(x) dx = \int_{-\infty}^\infty a(x(y)) \psi(y) dy, \quad (6)$$

where

$$\psi(y) = f_\nu(x(y)) \frac{dx(y)}{dy}.$$

Computational results show that the function ψ is unimodal for all positive integers ν . Let y^* denote the value of y at which $\psi(y)$ is maximized. We suppose, without loss of generality, that $|a(x)| \leq 1$ for all $x \in \mathbb{R}$.

Suppose that we are given the value $\epsilon > 0$ of a desired upper bound on the magnitude of the error of the approximation that we will develop. We now carry out the following two-step procedure.

Step 1 We will approximate (6) by

$$h \sum_{j=0}^{n-1} a(x(y_\ell + hj)) \psi(y_\ell + hj), \quad (7)$$

where n denotes the number of evaluations of the integrand $a(x(y)) \psi(y)$, $h = (y_u - y_\ell)/(n - 1)$ and y_ℓ and y_u are given numbers ($y_\ell < y^* < y_u$) such

that $y_u = y_\ell + h(n-1)$. We will choose n (and therefore h) via the progressive quadrature scheme described in Step 2.

In line with the recommendation of Press et al. (2007) that we try to arrange that the magnitudes of the discretization and trimming errors are approximately equal, we will choose y_ℓ and y_u such that the magnitude of

$$h \sum_{j=-\infty}^{-1} a(x(y_\ell + hj)) \psi(y_\ell + hj) + h \sum_{j=n}^{\infty} a(x(y_\ell + hj)) \psi(y_\ell + hj) \quad (8)$$

is guaranteed to be less than or equal to $\epsilon/2$. To do this, note that this magnitude is bounded above by

$$h \sum_{j=-\infty}^{-1} \psi(y_\ell + hj) + h \sum_{j=n}^{\infty} \psi(y_\ell + hj).$$

Consider

$$h \sum_{j=n}^{\infty} \psi(y_\ell + hj) = h \sum_{j=1}^{\infty} \psi(y_u + hj).$$

We now use the same reasoning as for the *integral test* for series convergence. Since $\psi(y_u + t)$ is a decreasing function of $t \geq 0$,

$$\begin{aligned} h \sum_{j=1}^{\infty} \psi(y_u + hj) &\leq \int_{y_u}^{\infty} \psi(t) dt = \int_{y_u}^{\infty} p_{\nu}(x(y)) \frac{dx(y)}{dy} dy \\ &= P(R > \nu^{1/2} x(y_u)) \\ &= 1 - Q_{\nu}(\nu x^2(y_u)), \end{aligned}$$

where Q_{ν} denotes the χ_{ν}^2 cdf. Similarly, since $\psi(y_\ell + t)$ is an increasing function of $t \in (-\infty, 0]$,

$$h \sum_{j=-\infty}^{-1} \psi(y_\ell + hj) \leq Q_{\nu}(\nu x^2(y_\ell)).$$

Therefore (8) has magnitude that is bounded above by

$$Q_{\nu}(\nu x^2(y_\ell)) + (1 - Q_{\nu}(\nu x^2(y_u))).$$

We require that y_ℓ and y_u ($y_\ell < y^* < y_u$) satisfy

$$Q_{\nu}(\nu x^2(y_\ell)) + (1 - Q_{\nu}(\nu x^2(y_u))) = \frac{\epsilon}{2}. \quad (9)$$

Of course, this does not uniquely specify (y_ℓ, y_u) . Define $\epsilon_\ell = Q_\nu(\nu x^2(y_\ell))$ and $\epsilon_u = 1 - Q_\nu(\nu x^2(y_u))$, so that

$$\epsilon_u = \epsilon/2 - \epsilon_\ell. \quad (10)$$

We can therefore express the problem of choosing (y_ℓ, y_u) as the problem of choosing $\epsilon_\ell \in (0, \epsilon/2)$, with ϵ_u then found from (10).

The inequality (3) suggests that it is reasonable to choose ϵ_ℓ such that $y_u - y_\ell$ is minimized, so that h is minimized for a given number of evaluations n . In other words, we minimize

$$y_u - y_\ell = x^{-1} \left(\left(\frac{Q_\nu^{-1}(1 - \epsilon/2 + \epsilon_\ell)}{\nu} \right)^{1/2} \right) - x^{-1} \left(\left(\frac{Q_\nu^{-1}(\epsilon_\ell)}{\nu} \right)^{1/2} \right)$$

with respect to $\epsilon_\ell \in (0, \epsilon/2)$.

Step 2

We choose n (and therefore h) in (7) using the following progressive quadrature procedure. Let $g(y) = a(x(y)) \psi(y)$. Suppose that the s 'th numerical approximation (starting with $s = 1$) to (1) is

$$I(s) = h(s) \sum_{j=0}^{n(s)-1} g(y_\ell + h(s)j),$$

where $h(s) = (y_u - y_\ell)/(n(s) - 1)$. In other words, $I(s)$ is based on $n(s)$ evaluations of the function g . The $(s + 1)$ 'th numerical approximation to (1) is

$$I(s + 1) = \frac{h(s)}{2} \sum_{j=0}^{n(s+1)-1} g \left(y_\ell + \frac{h(s)}{2} j \right),$$

where $n(s + 1) = 2n(s) - 1$. In other words, $I(s + 1)$ is based on $n(s + 1)$ evaluations of the function g . A convenient recursive formula for $I(s + 1)$ is

$$I(s + 1) = \frac{h(s)}{2} \sum_{j=0}^{n(s)-2} g \left(y_\ell + h(s)j + \frac{h(s)}{2} \right) + \frac{1}{2} I(s).$$

We iterate until

$$|I(s - 1) - I(s)| \leq \frac{\epsilon}{2}$$

When this condition is first satisfied we stop the iteration and use $I(s)$ as our final approximation. In other words, we use the simple approach to practical error estimation described on pp. 339–340 of Davis and Rabinowitz (1984).

4 Comparison with two other methods of numerical integration

In this section we use the simple test scenario that consists of evaluating a known univariate t probability. We compare the performance of the method described in the previous section with the two other methods described in the introduction.

Through the consideration of the coverage probability of a $1 - \alpha$ t-interval, it may be shown that

$$1 - \alpha = \int_0^\infty a_{\nu,\alpha}(x) f_\nu(x) dx, \quad (11)$$

where

$$a_{\nu,\alpha}(x) = 2 \Phi(t_{\nu,1-\alpha/2} x) - 1,$$

with Φ the $N(0,1)$ cdf and the quantile $t_{\nu,a}$ defined by $P(T \leq t_{\nu,a}) = a$ for $T \sim t_\nu$. Figure 1 provides an illustration of the fact that the $a_{\nu,\alpha}(x)$'s are smooth bounded functions of x for the values of α considered and all positive integers ν . This figure presents graphs of $a_{\nu,\alpha}(x)$ as a function of x for $\alpha = 0.05$ and $\nu = 1, 2$ and ∞ . The graph labeled $\nu = \infty$ refers to the case that $t_{\nu,1-\alpha/2}$ is replaced by its limit, as $\nu \rightarrow \infty$.

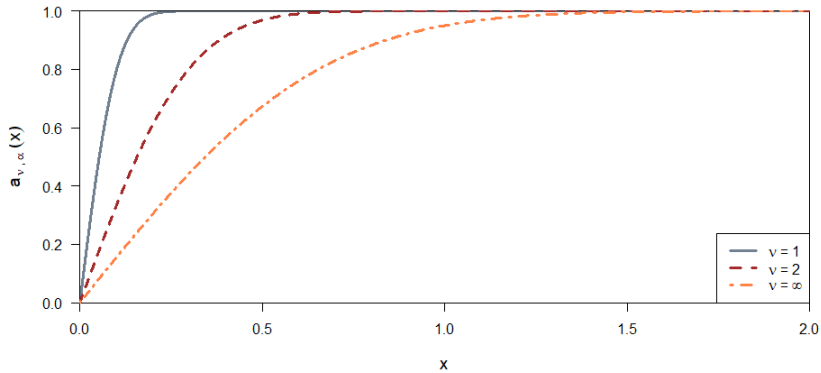


Figure 1: Graphs of $a_{\nu,\alpha}(x)$ as a function of x for $\alpha = 0.05$ and $\nu = 1, 2$ and ∞

4.1 “Mixed Rule” transformation, followed by the application of the trapezoidal rule

Apply the “Mixed Rule” transformation $x(y) = \exp(y - e^{-y})$, so that

$$\int_0^\infty a_{\nu,\alpha}(x) f_\nu(x) dx = \int_{-\infty}^\infty g_{\nu,\alpha}(y) dy, \quad (12)$$

where $g_{\nu,\alpha}(y) = a_{\nu,\alpha}(x(y)) \psi(y)$. Graphs of $g_{\nu,\alpha}(y)$ as a function of y are shown in Figure 2 for $\nu = 1, 3, 10$ and 100 and $\alpha = 0.10, 0.05$ and 0.02 . Each graph has a resemblance to the pdf of a normally distributed random variable, with increasing resemblance as ν increases. According to the heuristic described in the last paragraph of Section 2, we therefore expect the trapezoidal rule to be effective, with increasing efficiency as ν increases.

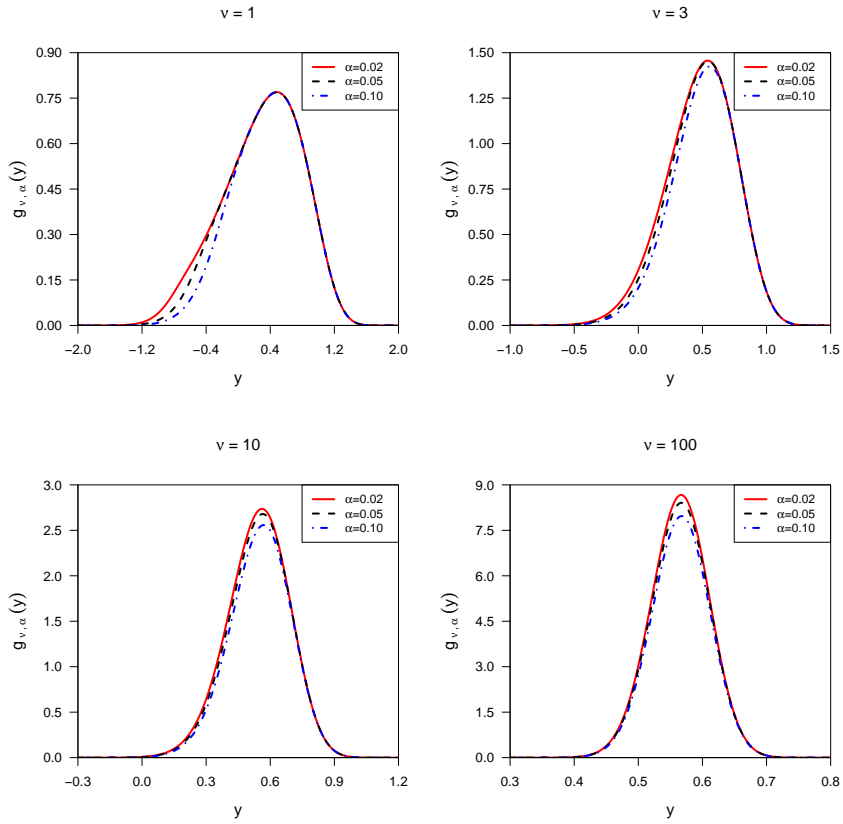


Figure 2: Graphs of $g_{\nu,\alpha}(y)$ as a function of y for $\nu = 1, 3, 10$ and 100 and $\alpha = 0.10, 0.05$ and 0.02

Define the approximation error to be the final approximation, obtained

using the two-step procedure described in Section 3, minus $1 - \alpha$. Table 1 presents the approximation error for $\alpha = 0.10, 0.05$ and 0.02 and $\nu = 1, 2, 3, 4, 5, 10, 100$ and 1000 , for $\epsilon = 10^{-6}$ and starting value $n(1) = 9$. Table 2 presents the total number of evaluations of the integrand $g_{\nu,\alpha}$ for these values of α, ν, ϵ and $n(1)$.

Table 1: The approximation error of the two-step procedure described in Section 3 for $\alpha = 0.10, 0.05$ and 0.02 and $\nu = 1, 2, 3, 4, 5, 10, 100$ and 1000 for $\epsilon = 10^{-6}$ and starting value $n(1) = 9$.

	$\nu = 1$	$\nu = 2$	$\nu = 3$	$\nu = 4$	$\nu = 5$
$\alpha = 0.10$	-8.27×10^{-8}	-2.08×10^{-8}	-2.86×10^{-8}	-3.63×10^{-8}	-4.40×10^{-8}
$\alpha = 0.05$	-8.27×10^{-8}	-2.08×10^{-8}	-2.88×10^{-8}	-3.69×10^{-8}	-4.52×10^{-8}
$\alpha = 0.02$	-8.27×10^{-8}	-2.08×10^{-8}	-2.91×10^{-8}	-3.78×10^{-8}	-4.69×10^{-8}
	$\nu = 10$	$\nu = 100$	$\nu = 1000$		
$\alpha = 0.10$	-7.73×10^{-8}	-1.59×10^{-7}	-1.73×10^{-7}		
$\alpha = 0.05$	-8.15×10^{-8}	-1.68×10^{-7}	-1.82×10^{-7}		
$\alpha = 0.02$	-8.69×10^{-8}	-1.75×10^{-7}	-1.87×10^{-7}		

Table 2: The total number of evaluations of the integrand $g_{\nu,\alpha}$ used for the computations listed in Table 1.

	$\nu = 1$	$\nu = 2$	$\nu = 3$	$\nu = 4$	$\nu = 5$	$\nu = 10$	$\nu = 100$	$\nu = 1000$
$\alpha = 0.10$	65	33	33	33	33	33	33	33
$\alpha = 0.05$	65	33	33	33	33	33	33	33
$\alpha = 0.02$	65	33	33	33	33	33	33	33

4.2 Generalized Gauss Laguerre quadrature

To apply Generalized Gauss Laguerre quadrature to the evaluation of (1), change the variable of integration to $y = \nu x^2/2$, so that

$$\int_0^\infty a(x) f_\nu(x) dx = \frac{1}{\Gamma(\nu/2)} \int_0^\infty d_\nu(y) c(y) dy,$$

where $c(y) = y^{(\nu/2)-1} \exp(-y)$ and $d_\nu(y) = a((2y/\nu)^{1/2})$. We then apply Generalized Gauss Laguerre quadrature, with m nodes (samples), to approximate

$$\int_0^\infty d_\nu(y) c(y) dy$$

by

$$\sum_{j=1}^m w_j d_\nu(y_j) \quad (13)$$

for the appropriately chosen w_j 's (which are all positive) and y_j 's ($0 < y_1 < \dots < y_m < \infty$). We define the approximation error to be (13) minus $1 - \alpha$.

Graphs of $d_\nu(y)$ as a function of y are shown in Figure 3 for $\nu = 1, 2, 3$ and 10 and $\alpha = 0.10, 0.05$ and 0.02 . It should be noted that the horizontal scales in each of the four panels of this figure are very different. It is known that Generalized Gauss Laguerre quadrature with m nodes will lead to the exact result if $d_\nu(y)$ is a polynomial in $y \in [0, \infty)$ of degree $2m - 1$ (Chandrasekhar, 1960, p.65).

We assess how well $d_\nu(y)$ can be approximated by a polynomial, over the finite interval of values of y such that $c(y)/\Gamma(\nu/2)$ is substantially greater than 0, as follows. Any polynomial p of degree u can be written as

$$p(y) = a_0 - \sum_{j=1}^u a_j (1 - y)^j.$$

Set $a_0 = 1$ and require that $\sum_{j=1}^u a_j = 1$, so that the functions p and d_ν take the same values at both $y = 0$ and $y = 1$. A first approximation to $d_\nu(y)$ by $p(y)$ over the interval $y \in [0, 1]$ is obtained by minimizing a measure of distance between $d_\nu(y)$ and $1 - (1 - y)^j$, over $j \in \{1, \dots, u\}$. A better approximation is obtained by minimizing a measure of distance between $d_\nu(y)$ and $1 - \sum_{j=1}^u a_j (1 - y)^j$, over a_1, \dots, a_u , subject to $\sum_{j=1}^u a_j = 1$. It follows from the shapes of the graphs in Figure 3 that to approximate $d_\nu(y)$ well by a polynomial, over the finite interval of values of y such that $c(y)/\Gamma(\nu/2)$ is substantially greater than 0, we would require this polynomial to be of very high degree, particularly for small ν . This suggests that Generalized Gauss Laguerre quadrature, with a given number of nodes m , will be most inaccurate for $\nu = 1$ and will have increasing accuracy as ν increases.

This suggested result is borne out by Table 3, which lists the approximation error for Generalized Gauss Laguerre quadrature for $\alpha = 0.10, 0.05$ and 0.02 and $\nu = 1, 2, 3, 4, 5, 6, 10, 100$ and 300 . We have chosen the number of nodes m to be the same as the number of integrand evaluations in Table 2. In other words, the number of nodes m is 65 for $\nu = 1$ and 33 for $\nu = 2, 3, 4, 5, 6, 10, 100$ and 300 .

Further confirmation of the unsuitability of Generalized Gauss Laguerre quadrature, in the scenario under consideration, for $\nu = 1$ and $\nu = 2$ is provided by Figure 4. The top and bottom panels of this figure are scatter-plots of the (y_j, w_j) 's for $(\nu, m) = (1, 65)$ and $(\nu, m) = (2, 33)$, respectively

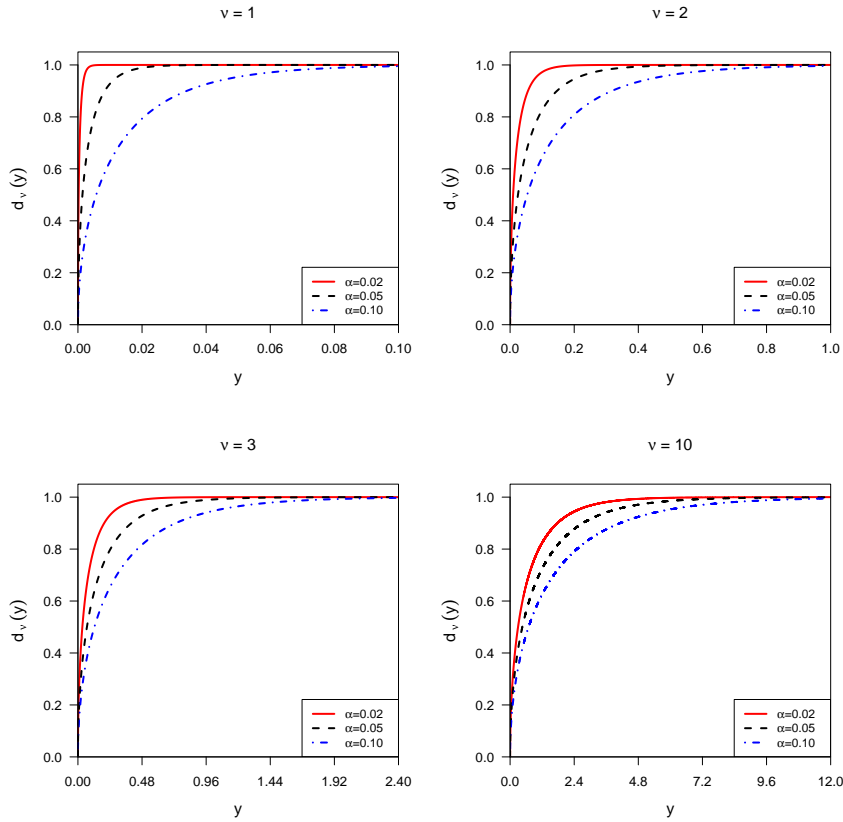


Figure 3: Graphs of $d_\nu(y)$ as a function of y for $\nu = 1, 2, 3$ and 10 and $\alpha = 0.10, 0.05$ and 0.02

$(y_j \leq 50)$. For $(\nu, m) = (1, 65)$ and $(\nu, m) = (2, 33)$ there are 30 values of $y_j > 50$ and 9 values of $y_j > 50$, respectively. When we compare the top panel of Figure 4 with the top left panel (the case $\nu = 1$) of Figure 3, we observe the following. Generalized Gauss Laguerre quadrature uses very few samples for the values of y where the function $d_\nu(y)$ is changing rapidly with increasing y , while using a large number of samples for values of y at which this function hardly changes with increasing y . Indeed, for $(\nu, m) = (1, 65)$ there are only 2 nodes in the interval $[0, 0.1]$. A similar conclusion results from comparing the bottom panel of Figure 4 with the top right panel (the case $\nu = 2$) of Figure 3. For $(\nu, m) = (2, 33)$ there are only 3 nodes in the interval $[0, 1]$.

Table 3: The approximation error for Generalized Gauss Laguerre quadrature for $\alpha = 0.10, 0.05$ and 0.02 and $\nu = 1, 2, 3, 4, 5, 6, 10, 100$ and 300 . The number of nodes m is 65 for $\nu = 1$ and 33 for $\nu = 2, 3, 4, 5, 6, 10, 100$ and 300 .

	$\nu = 1$	$\nu = 2$	$\nu = 3$	$\nu = 4$	$\nu = 5$
$\alpha = 0.10$	1.44×10^{-2}	1.32×10^{-3}	1.63×10^{-4}	2.86×10^{-5}	6.08×10^{-6}
$\alpha = 0.05$	3.25×10^{-2}	2.04×10^{-3}	2.26×10^{-4}	3.77×10^{-5}	7.84×10^{-6}
$\alpha = 0.02$	2.00×10^{-2}	4.12×10^{-3}	3.39×10^{-4}	5.24×10^{-5}	1.05×10^{-5}
	$\nu = 6$	$\nu = 10$	$\nu = 100$	$\nu = 300$	
$\alpha = 0.10$	1.48×10^{-6}	1.23×10^{-8}	-2.00×10^{-14}	-6.22×10^{-15}	
$\alpha = 0.05$	1.88×10^{-6}	1.52×10^{-8}	-2.11×10^{-14}	-6.21×10^{-15}	
$\alpha = 0.02$	2.46×10^{-6}	1.91×10^{-8}	-2.18×10^{-14}	-6.43×10^{-15}	

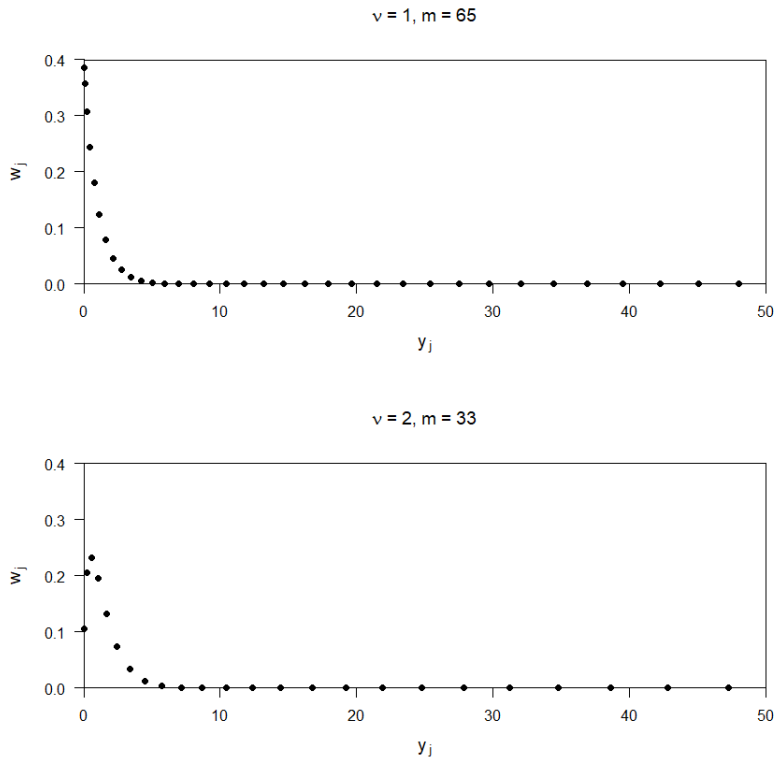


Figure 4: The top and bottom panels are scatterplots of the (y_j, w_j) 's for $(\nu, m) = (1, 65)$ and $(\nu, m) = (2, 33)$, respectively

Of course, one could greatly increase the number of nodes m and then approximate (13) by $\sum_{j=1}^q w_j d_\nu(y_j)$, where q is much less than m . This is unsatisfactory for the following two reasons. Firstly, the raison d'etre of Generalized Gauss Laguerre quadrature is that with m nodes it leads to the exact result for polynomials of degree $2m - 1$. This fundamental property is lost when this approximation is carried out. Secondly, this is a rather ad hoc way of forcing more samples of the function $d_\nu(y)$ into the quadrature formula for the values of y for which this function changes rapidly with increasing y .

4.3 Inverse cdf method

Change the variable of integration to $y = F_\nu(x)$, where F_ν denotes the cdf corresponding to the pdf f_ν , so that

$$\int_0^\infty a(x) f_\nu(x) dx = \int_0^1 a(F_\nu^{-1}(y)) dy.$$

A similar transformation is used, for example, by Genz and Bretz (2009, p.32). If desired, we can compute $F_\nu^{-1}(y)$ using either $F_\nu^{-1}(y) = (Q_\nu^{-1}(y)/\nu)^{1/2}$ or $F_\nu^{-1}(y) = F_R^{-1}(y)/\nu^{1/2}$, where F_R denotes the χ_ν cdf of R . We then change the variable of integration to $z = 2y - 1$ to obtain

$$\int_0^1 a(F_\nu^{-1}(y)) dy = \int_{-1}^1 b_\nu(z) dz,$$

where $b_\nu(z) = a(F_\nu^{-1}((z+1)/2))/2$. We then approximate the right-hand side, using Gauss Legendre quadrature with m nodes, by

$$\sum_{j=1}^m \tilde{w}_j b_\nu(z_j) \tag{14}$$

for the appropriately chosen \tilde{w}_j 's (which are all positive) and z_j 's ($-1 < z_1 < \dots < z_m < 1$). We define the approximation error to be (14) minus $1 - \alpha$.

Graphs of $b_\nu(z)$ as a function of z are shown in Figure 5 for $\nu = 1, 3, 10$ and 100 and $\alpha = 0.10, 0.05$ and 0.02 . It should be noted that the horizontal scale for the $\nu = 1$ panel is different from the horizontal scale for the $\nu = 3, 10$ and $\nu = 100$ panels (which are the same). It is known that Gauss Legendre quadrature with m nodes will lead to the exact result if $b_\nu(z)$ is a polynomial in $z \in [-1, 1]$ of degree $2m - 1$. When interpreting Figure 5, it is important to remember that $b_\nu(-1) = 0$ and that $b_\nu(z)$ is an increasing continuous function of $z \in [-1, 1]$. It is evident, then, from this figure that $b_\nu(z)$ increases very rapidly as z increases from zero for $\nu = 10$ and $\nu = 100$.

It follows from Figure 5 and the same kinds of considerations as in subsection 4.2 that the degree of the polynomial in z needed to approximate $b_\nu(z)$ well in the interval $z \in [-1, 1]$ increases with increasing ν . This suggests that the inverse cdf method, using Gauss Legendre quadrature with a given number of nodes m , will be most accurate for $\nu = 1$ and will have decreasing accuracy as ν increases.

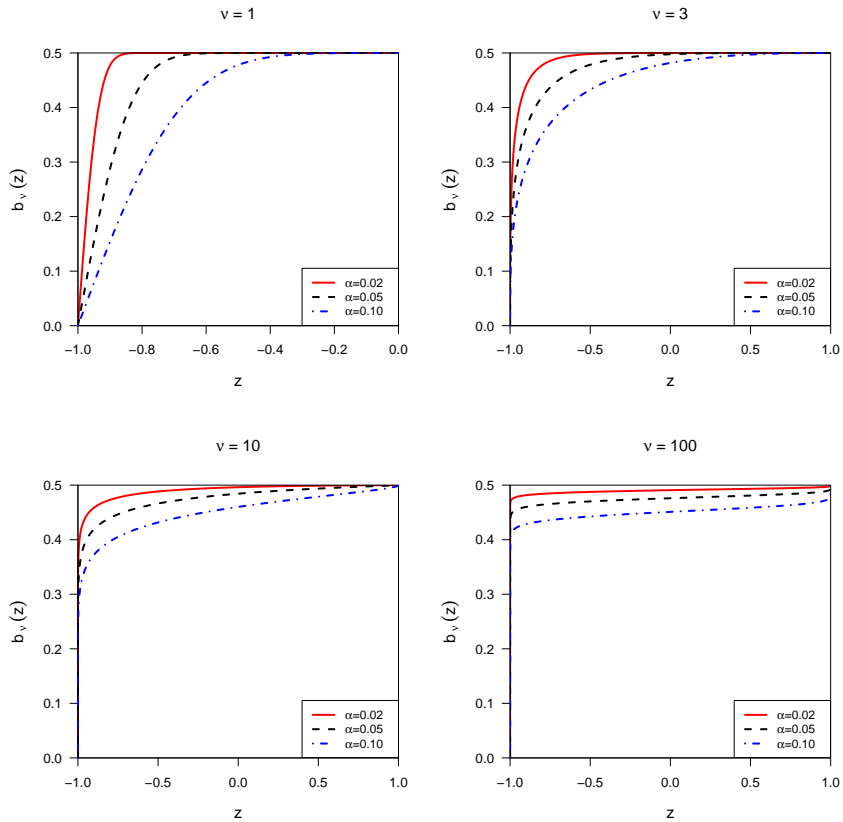


Figure 5: Graphs of $b_\nu(z)$ as a function of z for $\nu = 1, 3, 10$ and 100 and $\alpha = 0.10, 0.05$ and 0.02

This suggested result is borne out by the first 7 columns (the columns labelled $\nu = 1$ to $\nu = 10$) of Table 4, which lists the approximation error for Gauss Legendre quadrature for $\alpha = 0.10, 0.05$ and 0.02 and $\nu = 1, 2, 3, 4, 5, 6, 10, 100$ and 1000 . We have chosen the number of nodes m to be the same as the number of integrand evaluations in Table 2. In other words, the number of nodes m is 65 for $\nu = 1$ and 33 for $\nu = 2, 3, 4, 5, 6, 10, 100$ and 1000 .

Table 4: The approximation error for Gauss Legendre quadrature for $\alpha = 0.10, 0.05$ and 0.02 and $\nu = 1, 2, 3, 4, 5, 6, 10, 100$ and 1000 . The number of nodes m is 65 for $\nu = 1$ and 33 for $\nu = 2, 3, 4, 5, 6, 10, 100$ and 1000 .

	$\nu = 1$	$\nu = 2$	$\nu = 3$	$\nu = 4$	$\nu = 5$
$\alpha = 0.10$	7.77×10^{-16}	6.39×10^{-6}	1.52×10^{-5}	2.07×10^{-5}	2.37×10^{-5}
$\alpha = 0.05$	8.88×10^{-16}	9.43×10^{-6}	2.06×10^{-5}	2.70×10^{-5}	2.96×10^{-5}
$\alpha = 0.02$	8.88×10^{-16}	1.53×10^{-5}	2.94×10^{-5}	3.58×10^{-5}	3.75×10^{-5}
	$\nu = 6$	$\nu = 10$	$\nu = 100$	$\nu = 1000$	
$\alpha = 0.10$	2.47×10^{-5}	2.30×10^{-5}	4.01×10^{-6}	4.23×10^{-7}	
$\alpha = 0.05$	3.02×10^{-5}	2.64×10^{-5}	4.06×10^{-6}	4.23×10^{-7}	
$\alpha = 0.02$	3.68×10^{-5}	2.90×10^{-5}	3.36×10^{-6}	3.33×10^{-7}	

5 Application to the computation of the coverage probability and scaled expected volume of non-standard confidence regions

To assess the coverage probability and expected volume properties of the non-standard confidence regions considered in the references co-authored with Kabaila, one needs to evaluate integrals of the form (1). In this section we consider these types of evaluations in detail.

Kabaila and Giri (2009b), Kabaila and Giri (2009a), Kabaila and Tissera (2014) and Abeysekera and Kabaila (2017) need to evaluate integrals of the form

$$\int_0^\infty \lambda(x) x^\xi f_\kappa(x) dx$$

where ξ and κ are a positive integers and $\lambda : [0, \infty) \rightarrow \mathbb{R}$ is a smooth bounded function. This integral can be converted into the form (1) by changing the variable of integration to $y = c(\kappa, \xi) x$, where $c(\kappa, \xi) = (\kappa/(\kappa + \xi))^{1/2}$, so that

$$\int_0^\infty \lambda(x) x^\xi f_\kappa(x) dx = \left(\frac{2}{\kappa}\right)^{\xi/2} \frac{\Gamma(\nu/2)}{\Gamma(\kappa/2)} \int_0^\infty a(y) f_\nu(y) dy, \quad (15)$$

where $\nu = \kappa + \xi$ and $a(y) = \lambda(y/c(\kappa, \xi))$ is a smooth bounded function of $y \geq 0$.

In the references co-authored by Kabaila, the evaluation of (1) is required for given ν and for hundreds, or thousands or even tens of thousands of different functions a , all of which are smooth and bounded. In this case, the following “set-up costs” are negligible:

1. For the method described in Section 3 (application of the “Mixed Rule” transformation, followed by application of the trapezoidal rule), the “set-up cost” is computing y_ℓ and y_u .
2. For Generalized Gauss Laguerre quadrature, the “set-up cost” is computing the weights, w_j ’s, and nodes, y_j ’s, for this quadrature, followed by the computation of the $(2y_j/\nu)^{1/2}$ ’s
3. For the Inverse cdf method, the “set-up cost” consists of computing the weights, w_j ’s, and nodes, z_j ’s, for Gauss Legendre quadrature, followed by the computation of the $F_\nu^{-1}((z_j + 1)/2)$ ’s.

In other words, the number of evaluations of the function a provides a reasonable guide to the computational effort for each of these methods.

In the Supplementary Material, we illustrate the application of the method described in Section 3 to the computation, using a formula closely related to (1) of Kabaila and Giri (2009b), for the coverage probability of a particular post-model-selection confidence interval. This formula requires the evaluation of an integral of the form (1) that, after the “Mixed Rule” transformation, becomes

$$\int_{-\infty}^{\infty} \tilde{g}_{\nu,\alpha}(y) dy,$$

where, in addition to ν and α , the function $\tilde{g}_{\nu,\alpha}$ is determined by the quantities $\tilde{\alpha}$, γ and ρ . Graphs of $\tilde{g}_{\nu,\alpha}(y)$ as a function of y are shown in Figure 6 for $\nu = 2, 3, 10$ and 100 , $\alpha = 0.10, 0.05$ and 0.02 , $\tilde{\alpha} = 0.1$, $\gamma = 2$ and $\rho = 0.8$.

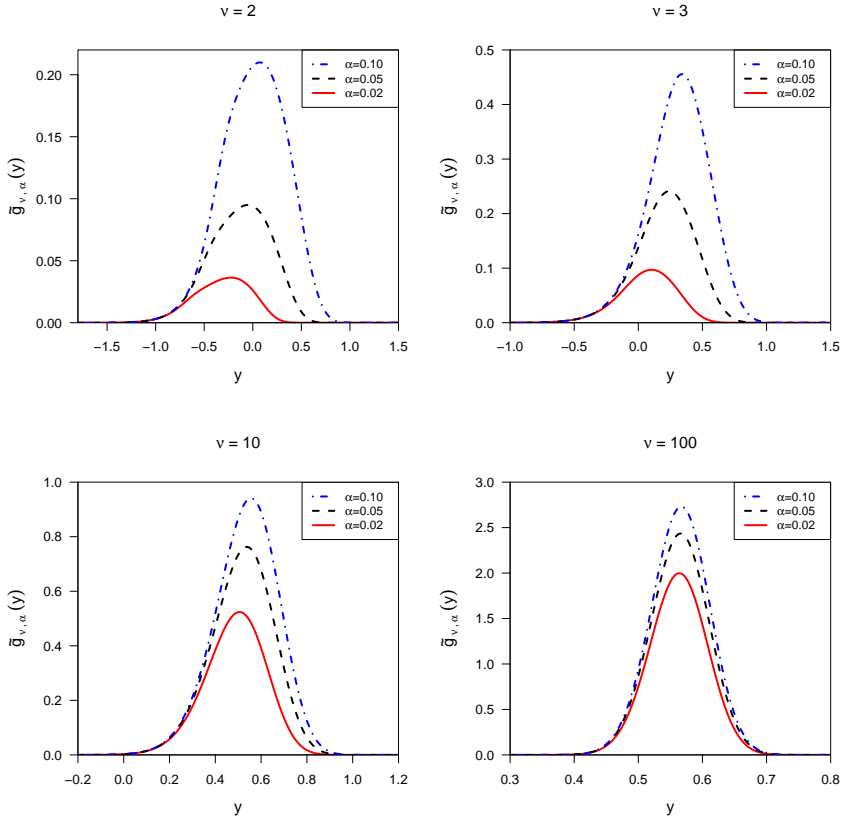


Figure 6: Graphs of $\tilde{g}_{v,\alpha}(y)$ as a function of y for $\nu = 2, 3, 10$ and 100 , $\alpha = 0.10, 0.05$ and 0.02 , $\tilde{\alpha} = 0.1$, $\xi = 1$, $\gamma = 2$ and $\rho = 0.8$

Each graph in Figure 6 has a resemblance to the pdf of a normally distributed random variable. According to the heuristic described in the last paragraph of Section 2, we therefore expect the trapezoidal rule to be effective. In the Supplementary Material we extensively analyse the accuracy of the method described in Section 3 and show that it performs well.

6 Discussion

In Section 4, for each of the three methods of numerical integration, we present graphs whose features accurately predict their performance in terms of accuracy for a given number of evaluations of the function a . As noted in Section 5, the number of evaluations of the function a is a reasonable measure of computational effort when the “set-up costs” are negligible, as in the situations considered by Kabaila and co-authors.

Our findings for the test scenario considered in Section 4 are as follows. The Generalized Gauss Laguerre quadrature method performs worst for $\nu = 1$, and has performance that improves with increasing ν . It has the worst performance of the three methods for $\nu = 1, 2$ and 3 . The inverse cdf method performs best for $\nu = 1$, and has performance that decreases as ν increases through the values $2, 3, 4, 5, 6$ and 10 . The inverse cdf method is the best performing of the three methods for $\nu = 1$. The method described in Section 3 (application of the ‘‘Mixed Rule’’ transformation, followed by application of the trapezoidal rule) performs more or less equally well for all of the values of ν considered, namely, $\nu = 1, 2, 3, 4, 5, 10, 100$ and 1000 . It has the best performance of the three methods for $\nu = 2, 3, 4, 5$ and 10 . For many of the situations considered by Kabaila and co-authors, the smallest possible value of ν , in the evaluation of integrals of the form (1), is 2 .

The method described in Section 3 uses a nested sequence of quadrature rules, for the estimation of the approximation error, so that previous evaluations of the function a are not wasted. This nested sequence can be implemented in a very simple computer program. This is an important advantage of this method over the other two methods. The numerical results reported in the Supplementary Material support our overall belief that the method described in Section 3 will be very useful for many of the situations considered by Kabaila and co-authors.

Acknowledgement

This work was supported by an Australian Government Research Training Program Scholarship.

Appendix: Computation of the inverse of the function x

Define the function $x : (0, \infty) \rightarrow \mathbb{R}$ by $x(y) = \exp(y - e^{-y})$ for all $y > 0$. To compute $x^{-1}(z)$, for given $z > 0$, we solve

$$\ln(z) = y - e^{-y}$$

for y . To compute y using the R function `uniroot`, we use the following finite bounds on $x^{-1}(z)$:

1. For $\ln(z) \leq -1$: $\max(\ln(z), -\ln(-\ln(z))) \leq x^{-1}(z) \leq -\ln((1 - \ln(z))/2)$.
2. For $\ln(z) > -1$: $\max(0, \ln(z)) \leq x^{-1}(z) \leq \ln(z) + 1$.

The proof of these bounds is omitted for the sake of brevity.

References

Abeysekera, W., Kabaila, P., 2017. Optimized recentered confidence spheres for the multivariate normal mean. *Electronic Journal of Statistics* 11, 1935–7524.

Chandrasekhar, S., 1960. Radiative transfer. Dover, New York.

Davis, P.J., Rabinowitz, P., 1984. Methods of numerical integration, 2nd ed. Academic Press, San Diego, CA.

Dunnett, C.W., 1989. Algorithm as 251: Multivariate normal probability integrals with product correlation structure. *Journal of the Royal Statistical Society, Series C (Applied Statistics)* 38, 564–579.

Dunnett, C.W., Sobel, M., 1955. Approximations to the probability integral and certain percentage points of a multivariate analogue of student's t-distribution. *Biometrika* 42, 258–260.

Farchione, D., Kabaila, P., 2008. Confidence intervals for the normal mean utilizing prior information. *Statistics and Probability Letters* 78, 1094–1100.

Genz, A., Bretz, F., 2009. Computation of multivariate normal and t probabilities. Springer, London.

Gupta, S.S., Panchapakesan, S., 2002. Multiple decision procedures: theory and methodology of selecting and ranking populations. SIAM, Philadelphia.

Hardy, G.H., 1933. A theorem concerning Fourier transforms. *Journal of the London Mathematical Society* 8, 227–231.

Hochberg, Y., Tamhane, A.C., 1987. Multiple comparison procedures. Wiley, New York.

Kabaila, P., 2018. On the minimum coverage probability of model averaged tail area confidence intervals. *Canadian Journal of Statistics* 46, 279–297.

Kabaila, P., Farchione, D., 2012. The minimum coverage of confidence intervals in regression after a preliminary F test. *Journal of Statistical Planning and Inference* 142, 956–964.

Kabaila, P., Giri, K., 2009a. Confidence intervals in regression utilizing uncertain prior information. *Journal of Statistical Planning and Inference* 139, 3419–3429.

Kabaila, P., Giri, K., 2009b. Upper bounds on the minimum coverage probability of confidence intervals in regression after model selection. *Australian & New Zealand Journal of Statistics* 51, 271–287.

Kabaila, P., Tissera, D., 2014. Confidence intervals in regression that utilize uncertain prior information about a vector parameter. *Australian & New Zealand Journal of Statistics* 56, 371–383.

Kabaila, P., Welsh, A.H., Abeysekera, W., 2016. Model-averaged confidence intervals. *Scandinavian Journal of Statistics* 43, 36–48.

Kabaila, P., Welsh, A.H., Mainzer, R., 2017. The performance of model averaged tail area confidence intervals. *Communications in Statistics - Theory and Methods* 46, 10718–10732.

Mi, X., Miwa, T., Hothorn, T., 2009. mvtnorm: new numerical algorithm for multivariate normal probabilities. *R Journal* 1, 37–39.

Miller, R.G., 1981. *Simultaneous statistical inference*, 2nd ed. Springer, New York.

Miwa, T., Hayter, A.J., Kuriki, S., 2003. The evaluation of general non-centred orthonormal probabilities. *Journal of the Royal Statistical Society, Series B* 65, 223–234.

Mori, M., 1985. Quadrature formulas obtained by variable transformation and the de-rule. *Journal of Computational and Applied Mathematics* 12 & 13, 119–130.

Papoulis, A., 1962. *The Fourier integral and its applications*. McGraw-Hill, New York.

Press, W.H., Teukolsky, S.A., Vetterling, W.T., Flannery, B.P., 2007. *Numerical recipes: the art of scientific computing*, 3rd ed. Cambridge University Press, Cambridge.

Takahasi, H., Mori, M., 1973. Quadrature formulas obtained by variable transformation. *Numerische Mathematik* 21, 206–219.

Trefethen, L.N., Weideman, J.A.C., 2014. The exponentially convergent trapezoidal rule. *SIAM Review* 56, 385–458.